ACS POLYMERS Au
AN OPEN ACCESS JOURNAL OF THE AMERICAN CHEMICAL SOCIETY

pubs.acs.org/polymerau

Article

Utility of Chemical Upcycling in Transforming Postconsumer PET to PBT-Based Thermoplastic Copolyesters Containing a Renewable Fatty-Acid-Derived Soft Block

Apostolos A. Karanastasis, Victoria Safin, Subin Damodaran, and Louis M. Pitet*

Cite This: *ACS Polym. Au* 2022, 2, 351–360

Read Online

ACCESS | Metrics & More | Article Recommendations | Supporting Information

ABSTRACT: Thermoplastic copolyesters (TPCs) are important structural components in countless high performance applications that require excellent thermal stability and outstanding mechanical integrity. Segmented multiblock architectures are often employed for the most demanding applications, in which semicrystalline segments of poly(butylene terephthalate) (PBT) are combined with various low T_g soft blocks. These segmented copolymers are nearly always synthesized from pristine feedstocks that are derived from fossil-fuel sources. In this work, we show a straightforward, one-pot synthetic approach to prepare TPCs starting from high-molar mass poly(ethylene terephthalate) recyclate (rPET) combined with a hydrophobic fatty acid dimer diol flexible segment. Transesterification is exploited to create a multiblock architecture. The high molar mass and segment distribution are elucidated by detailed size-exclusion chromatography and proton and carbon nuclear magnetic resonance spectroscopy. It is also shown that rPET can be chemically converted to PBT through a molecular exchange, in which the ethylene glycol is substituted by introducing 1,4-butane diol. A series of copolymers with various compositions was prepared with either PET or PBT segments and the final thermal properties and mechanical performance is compared between the two different constructs. Ultimately, PBT-based TPCs crystallize faster and exhibit a higher modulus over the range of explored compositions, making them ideal for applications that require injection molding. This represents an ideal, sustainable approach to making conventional TPCs, utilizing recyclate and biobased components to produce high performance polymer constructs via an easily accessible upcycling route.

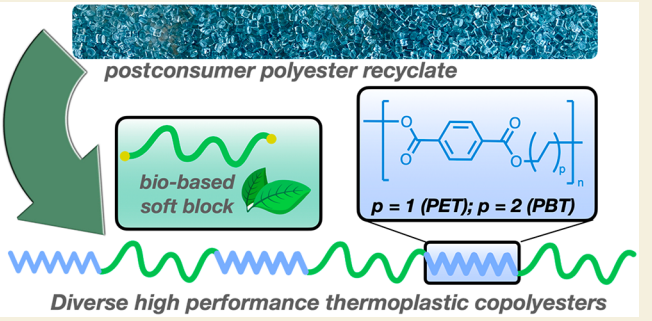

KEYWORDS: *thermoplastic copolyesters, recycling, upcycling, condensation polymers, plastic reutilization, biobased building blocks*

INTRODUCTION

There is growing scrutiny over what can be done to rectify the global plastic pollution crisis, which has arisen from the unabated growth in plastic production over the last decades.[1] Under current levels of recycling and a business-as-usual approach, the contribution of plastics production to climate change and ecological destruction is projected to worsen substantially.[2−4] Polyethylene terephthalate (PET) is a high volume waste stream—tens of millions of tons are produced annually and are used in several environmentally problematic markets including bottles and textiles, which are discarded after remarkably short useful lifetimes. While recycling has improved over the years, there is still a dire need for improving the number of outlets for reutilizing this potentially valuable resource.[5−9] There is tremendous potential in uncovering routes toward high-value materials by chemically transforming various plastic waste streams in so-called upcycling processes.[10−16] Utilizing PET recyclate (rPET) through chemical diversification has found some traction. Typically, rPET is chemically depolymerized in an initial step, followed by repolymerization with various comonomers to form copolymers.[17] Alternatively, rPET has been reacted directly with various functional building blocks to form diverse copolyesters, plasticizers, or resins.[18−20] This has been done with several biobased bifunctional comonomers such as isosorbide[21,22] or fatty acid derivatives,[23,24] but this approach routinely leads to oligomers lacking mechanical integrity. Our interest lies in generating high molar mass segmented copolymers, generically called thermoplastic copolyesters (TPCs) possessing high-performance mechanical properties, using a direct, one-pot reaction pathway from rPET.[25]

TPCs are multiblock copolymers comprising alternating rigid and flexible segments.[26,27] They are found in an enormous array of engineering plastic applications, owing to

Received: May 5, 2022
Revised: June 22, 2022
Accepted: June 23, 2022
Published: July 7, 2022

Scheme 1. Complementary Synthetic Pathways to Segmented Copolyesters by Combining rPET with Renewable FADD Soft Block to Form Either PET-FADD Copolyesters (Top) or PBT-FADD Copolyesters (Bottom) through Chemical Exchange

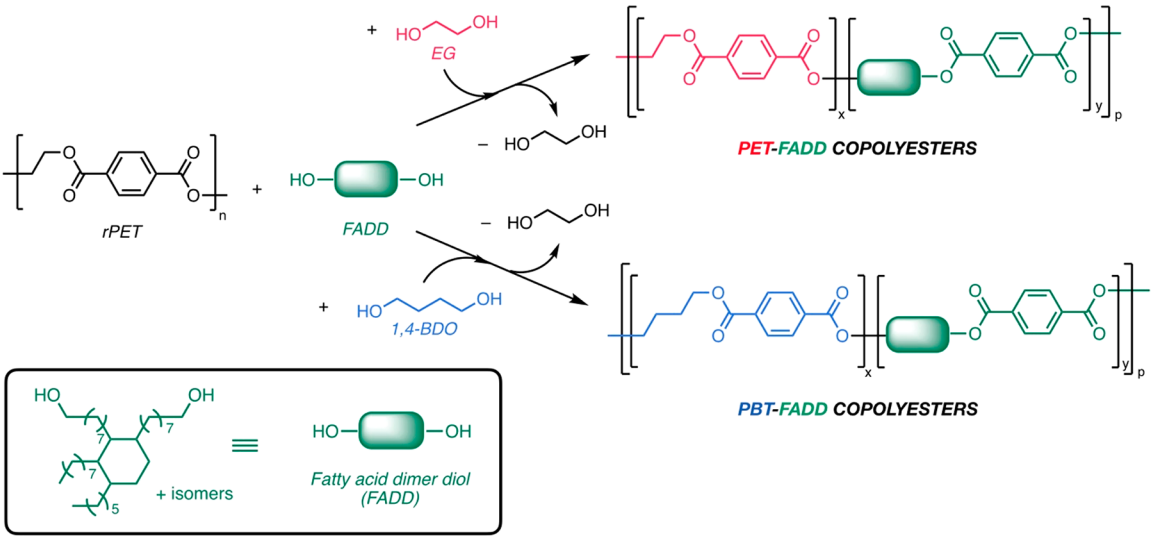

the broad range of accessible properties.[28] The rigid segment in TPCs is typically a semicrystalline or glassy polyester.[29] The flexible counterpart in TPCs is typically a long chain polyol (500−3000 g/mol) having a low glass transition temperature (T_g).[30,31] The primary handles for fine-tuning the final properties include the composition (i.e., soft/hard ratio), the polyol molar mass, and the chemo-mechanical properties of the soft block. Significant attention has been given to preparing these high-performance materials from more sustainable feedstocks. Several different biobased rigid segments have been explored, which have a profound impact on the final properties.[32] Likewise, a number of different renewable, bio-derived long-chain soft-blocks have been employed as building blocks in TPCs. One of the more appealing, and commercially available, flexible bifunctional units is based on dimerized fatty (linoleic) acids, or fatty acid dimer (FADs).[33−35] Functional derivatives of FADs have been used in various thermoplastic constructs, relying on the bifunctionality for step-growth processes.[36−38] Aside from being from renewable origins, the FADD building blocks offers appealing property aspects, particularly with respect to its hydrophobic character and short chain branching. These structural attributes can impart highly attractive surface and barrier properties, including resistance to hydrolytic degradation, as well as favorable processing during molding, for example.

In many TPC variants that are commercially available, the hard, semicrystalline segments are poly(butylene terephthalate) (PBT). PBT makes an essential contribution to the outstanding mechanical properties typically exhibited in these materials, due to the strong physical cross-linking and extensive crystallinity. PBT is almost exclusively employed as a hard segment in commercial analogs of TPCs because of its well-recognized fast crystallization, making it an ideal candidate for injection molded parts where fast production cycles and rapid cooling are essential.[39,40] In fact, fatty acid dimer diol (FADD) derivatives have been incorporated as soft segments in PBT-based TPCs via conventional melt-polymerization and solid-state polycondensation.[41−44] These examples serve as important indicators for the appealing properties of such constructs. However, we aim to demonstrate accessibility to comparable properties starting from responsibly sourced feedstocks (i.e., recyclate and renewables) with an innovative synthetic approach.

Here we show the direct upcycling of postconsumer rPET, transforming it into high value TPCs through combination with a biobased renewable FADD. Virgin PET routinely sells for approximately 1 €/kg, while the market price for various TPCs is appreciably higher (2−5×). TPCs are typically used in higher-end applications that have more demanding property profiles, such as automotive parts, consumer electronics, and medical devices (see, for example, https://www.dupont.com/brands/hytrel.html). Our strategy involves using complementary routes, showing the versatility in the final chemical structure by including two different small molecule diols as reactive comonomers. Along one avenue, ethylene glycol (EG) is added to generate PET-FADD segmented copolyesters (Scheme 1, top). In parallel, 1,4-butanediol (BDO) was added as reactive comonomer, which generates analogous PBT-FADD copolyesters upon substitution into the rPET backbone (Scheme 1, bottom). The different copolymers are interrogated thoroughly to uncover contrasting thermal and mechanical properties, which are connected to the detailed molecular makeup as confirmed with various analytical tools. This work builds on our previous publication in two important ways.[25] First, a functional fatty acid diol is used in place of a diacid. This has significant implications in the molecular structure of the corresponding repeating unit. The diol is complemented by a terephthalate unit in each repeating unit, offering potentially enhanced stability from the corresponding semiaromatic esters. Second, and more importantly, we here show the versatility of the up-cycling concept by chemically transforming the engineering (hard) polyester block from PET to PBT through an innovative chemical exchange performed in situ.

RESULTS AND DISCUSSION

Synthesis of TPCs

The TPC copolymers prepared in this work were all made using a one-pot melt polycondensation, where all ingredients are introduced into a single, specialized reactor flask (Figure S2). All of the copolymers in this work were constructed using

https://doi.org/10.1021/acspolymersau.2c00019
ACS Polym. Au 2022, 2, 351−360

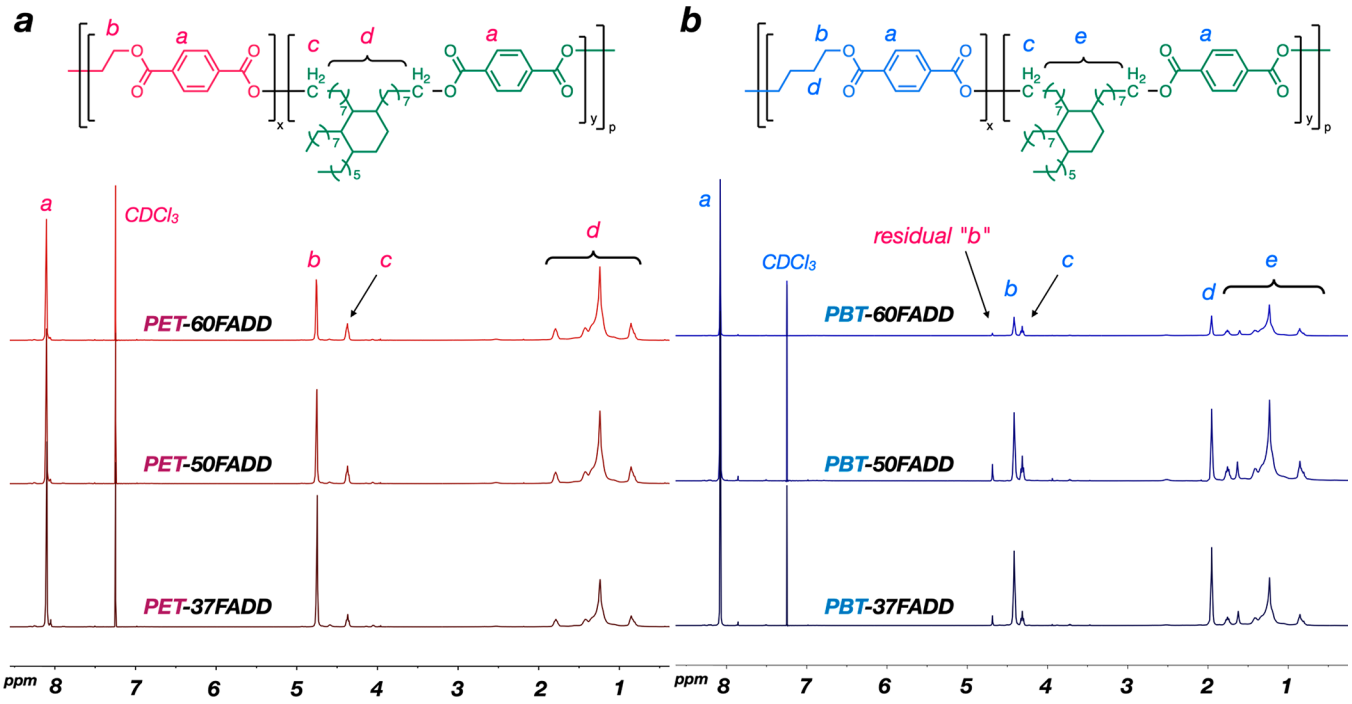

Figure 1. Representative ^{1}H NMR spectra of TPCs synthesized from each sample from the series (a) PET-FADD and (b) PBT-FADD.

a fatty acid dimer diol (FADD) as the major soft-block constituent (Scheme 1). This diol is a hydrophobic telechelic unit with an average molar mass of ∼550 g/mol. The product is prepared via the dimerization of linoleic acid followed by hydrogenation. The product is supplied from Croda under the trade name Pripol 2033. It contains a variety of different isomers from the dimerization process, but the predominant structure is that shown in Scheme 1. Critically, the functionality (F_n) of the end product mixture is highly controlled at a value of 2.0 (see Supporting Information, Figure S1 for a structural overview). Thus, FADD is perfectly suited for use in this polycondensation/transesterification process and will not lead to extensive branching or chain capping in the step-growth polymerization process. The telechelic FADD is combined with high molar mass (M_n ∼ 25 kg/mol) postconsumer rPET recyclate, which undergoes transesterification to yield extensive chain scission in the rPET and ultimately form a segmented copolymer. The recipes are modified depending on the target copolymer and composition. Two separate complementary series of segmented copolyesters were synthesized, each individual copolymer having a specific target soft-to-hard ratio (i.e., composition).

The first series includes rPET, FADD, and excess ethylene glycol (EG) in the recipe, in addition to transesterification catalyst titanium tetrabutoxide (TBT). This approach was found to be optimal in obtaining randomized segment distributions in the final polymer constructs. The EG acts to promote rapid in situ depolymerization of the PET, offering a significant concentration of hydroxyl end-groups that are ultimately responsible for the repeating unit redistribution. In the absence of EG, and thus inadequate −OH concentrations, the essential transesterification reaction is simply too slow, owing to the relatively high molar mass of FADD. At the high temperatures required for melt polycondensation with rPET (∼250 °C; see the Supporting Information for detailed synthetic steps), polymer degradation is in competition with the polycondensation responsible for chain elongation. Thus, EG is a reactant that accelerates the randomization via transesterification and favors relatively rapid depolymerization. After initial depolymerization/transesterification aided by the EG in the first stage of the melt polymerization, the temperature is increased and low vacuum (10^{-3} mbar) is applied to recuperate the EG through further trans reactions, accompanied by an increase in molar mass. The final polymer structure comprises rigid blocks of PET repeating units and flexible blocks of FADD-terephthalate repeating units (Scheme 1, top).

The second series was prepared utilizing a similar strategy for promoting extensive in situ depolymerization. However, excess 1,4-butane diol (BDO) was added in place of EG, acting in this case as the critical source of hydroxyl group reactants that participate directly as reactant in the molecular exchange via transesterification with the rPET backbone. In this case, the more volatile EG (bp 197 °C) is selectively distilled and removed from the reactor under vacuum. Meanwhile, the less volatile BDO (bp 230 °C) exchanges with the EG, substituting itself into the polymer backbone to form repeating units of PBT. The amount of excess BDO was optimized in order to achieve the near−complete exchange of EG within a comparable reaction time to the first series of copolymers (see the Supporting Information for detailed recipes). The final polymer construct is thus analogous, with the rigid segment now comprising PBT and having an identical flexible segment repeat unit structure (Scheme 1, bottom). The molecular exchange of EG with BDO has been reported for the transformation of homopolymer PET to homopolymer PBT, providing useful guidance in terms of optimized temperature profiles and catalyst.[45]

Each of the two series contain three samples with variable composition, which was achieved by judiciously adjusting the feed ratios of starting materials. The first series is named PET-XXFADD, where XX indicates the final weight percent of the

https://doi.org/10.1021/acspolymersau.2c00019
ACS Polym. Au 2022, 2, 351−360

Table 1. Molecular Characteristics of the PET- and PBT-Based Copolyesters from ^{1}H NMR Spectroscopy and SEC Measurements

				RI detection[d]			light scattering detection[e]		
entry	wt % SB (target)[a]	wt % SB (expt)[b]	mol % HB from EG[c]	M_n (kg/mol)	M_w (kg/mol)	$Đ$	M_n (kg/mol)	M_w (kg/mol)	$Đ$
PET-37DFA	37	38.5	100	18.0	60.9	3.4	44.3	65.1	1.5
PET-50DFA	50	50.3	100	19.8	92.2	4.8	46.5	86	1.8
PET-60DFA	60	61.4	100	30.7	121	4.0	50.1	103	2.0
PBT-37DFA	37	35.8	4.8	18.4	73.5	4.0	45.7	66.4	1.5
PBT-50DFA	50	50.1	8.9	18.4	88.8	4.5	43.3	70.5	1.6
PBT-60DFA	60	60.7	5.4	25.4	119	4.2	52.5	96	1.8

[a]Target wt % soft block based on the recipe and assuming 100% incorporation of the FADD flexible diol. [b]Experimental wt % determined from relative integration of the FADD repeat units and the hard block (PET or PBT) repeat units in ^{1}H NMR spectra. [c]mol % Hard block from EG determined from the integration of signals attributed to EG (i.e., PET) compared with those from BDO (i.e., PBT). [d]Determined by SEC, relative to polystyrene standards in chloroform. [e]Determined by SEC using multiangle (3-angle) light scattering detection, where the dn/dc was determined assuming 100% sample elution.

FADD-terephthalate segment. Three samples were prepared with targets of 37, 50, and 60 wt % FADD repeating units, as verified by ^{1}H NMR spectroscopy (vide infra). The second series is named PBT-XXFADD, with complementary amounts of soft block (i.e., 37, 50, 60 wt %). All reactions were carried out on a custom-built melt polymerization reactor with a 1 L internal reactor volume (Figure S2). Equal final masses of polymers were targeted for each sample. The unique melt reactor is equipped with a mechanical stirrer that monitors torque throughout the reaction. The torque on the stirrer is proportional to the melt viscosity (η) of the reaction mixture, which gradually increases as condensate is removed, signaling an evolution of molar mass. Having equal mass of product normalizes the viscosity, and the reaction is terminated at approximately the same torque readout of 35 N cm at the same stirring rate of 25 rpm (i.e., approximately constant shear rate). The product was removed from the reactor and rapidly cooled by submerging in deionized water. Each sample was finally dried in a vacuum oven before analyzing for molecular, thermal and mechanical characteristics.

Molecular Analysis of TPCs

The molecular makeup was elucidated with ^{1}H NMR spectroscopy for both series of copolymers (Figure 1). Solutions were prepared with a 90:10 mixture of $CDCl_3$ and deuterated trifluoroacetic acid, to aid with miscibility compared with pure chloroform. The spectra reveal several important structural aspects. First, the relative ratio of hard block and soft block are easily calculated based on the well-resolved signals from the respective segments (Table 1). Both series of copolymers contain distinct aromatic signals arising from units in both soft and hard blocks. Likewise, the aliphatic protons from the FADD units are both easily identifiable in the region between 0.5 and 1.8 ppm. The methylene-ester protons (proton c in the PET-based and PBT-based copolymers, respectively) on the aliphatic FADD repeat units consistently appears at 4.3 ppm. The disappearance of the methylene signals adjacent to the hydroxyl groups in the starting FADD strongly supports the participation in transesterification, and thus subsequent inclusion into the segmented copolyester structure. The relevant signals clearly shift from 3.6 ppm in the starting diol to 4.3 ppm in the copolyesters (Figure S3, Figure 1). The PET-based copolymers have one clear signal from the ethylene units in the hard block (signal b), whereas the PBT-based copolymers have two signals from butyl units in the hard block (signal b and c). Critically, the spectra in the PBT-based copolymers are consistent with nearly quantitative substitution of BDO with EG in the backbone structure of the copolyester. However, there are low levels of residual EG remaining in each sample, as suggested by the signal at 4.65 ppm. Calculating the amount of EG relative to BDO incorporation reveals between 5−10% of PET repeat units remain with respect to overall hard block (Table 1). Obtaining copolymers with complete replacement of EG with a less volatile substitute is prohibitive, balancing total reaction time with competing degradation that can occur at the relatively high reaction temperatures. However, the relatively low levels of EG remaining do not appreciably influence the macroscopic thermal or mechanical characteristics (vide infra).

In each sample, the overall composition has been determined from the spectra and reported in terms of wt % soft-block, taking into account the entire soft block repeat units (i.e., FADD + TP). The target values based on recipe as well as the experimentally determined values from NMR spectroscopy reflect a strongly consistent feed−product relationship (Table 1). Further analysis of the segment makeup and segment distribution was extracted from ^{13}C NMR spectroscopy, wherein the decoupled signals from the aromatic carbons reveals the quantity of different dyad sequences (Figure S4).[43] The aromatic region reveals signals consistent with nearly quantitative transformation of PET repeating units to PBT. Additionally, the calculated randomness values reveal nearly fully random distributions (R = 0.8−1.0), corresponding to extensive transesterification during the molecular exchange (Table S2). However, the PBT-based samples notably contain a small quantity of ETE dyads (from residual PET repeating units) and have marginally lower randomness values. This is in line with the proton NMR spectra. The small signal in the ^{13}C spectra appearing near 134 ppm in all three samples of PBT-FADD copolymers is consistent with small amounts of residual EG. The magnitude is also consistent with the relative quantities of residual EG calculated from the proton spectra.

The melt polycondensations were conducted in a custom-built reactor equipped with a torque gauge (Figure S2). Each sample had approximately the same target mass, and thus, torque is directly linked to the melt viscosity. Each reaction was stopped at an approximate torque of 35 N cm. The resulting products were prepared as a dilute solution in chloroform for chromatographic analysis. The samples were injected onto SEC columns running on pure chloroform and the resulting chromatograms were analyzed for molar mass and dispersity relative to polystyrene (PS) standards from a refractive index detector (Figure S5) and with a multiangle

https://doi.org/10.1021/acspolymersau.2c00019
ACS Polym. Au 2022, 2, 351−360

light scattering detector (Figure 2). According to the refractive index detector, all samples exhibit product distributions

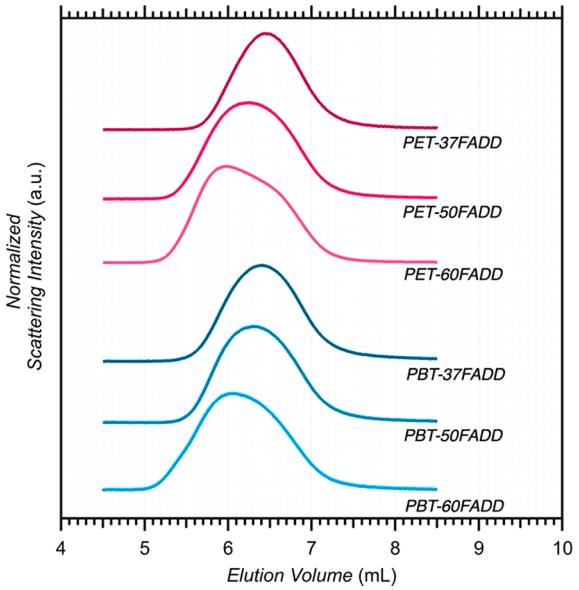

Figure 2. Molecular weight distributions of samples from SEC measurements performed in chloroform at 40 °C, with data from light scattering detection shown.

consistent with high molar mass, with peak distributions centered between 60−70 kg/mol using the calibration curve created from PS standards. Surprisingly, the distributions are all relatively broad, with dispersities ($Đ$) being significantly higher than expected for conventional step-growth, linear polymer architectures (Table 1; RI detection). This spurred our interest in analyzing the sample distributions with a light scattering detector, extracting the absolute molar mass and dispersity. Exact sample concentrations were carefully measured and 100% sample elution volume was assumed in order to determine the refractive index increment (dn/dc) in situ. Despite the fact that the actual distributions (i.e., the chromatograms) are not dramatically different visually compared with RI detection, the dispersity and molar mass differ considerably (Table 1; light scattering detection). The large differences are not wholly surprising, as the architecture and corresponding free-volume of the complex copolyesters compared with linear polystyrene standards will have profoundly different solution conformations. In particular, the dispersities measured by light scattering range from 1.5−2.0, which is closer in line with expectations based on the step-growth mechanism. This further suggests that the architectures are predominantly linear, absent of substantial side reactions that would lead to extensive long-chain branching. Incidentally, the rPET has a molar mass M_n of ca. 20 kg/mol according to the supplier, which is consistent with the source of postconsumer bottles.[46] The molar mass is strictly regulated, and typically tailored to an industry-standard intrinsic viscosity value of 0.65 dL/g (see the Supporting Information for details on rPET supply). Chromatograms of rPET are not included here because of the insolubility in chloroform, and thus incomparability with the TPCs. Nevertheless, the exact molar mass of the rPET should not have a substantial influence on the depolymerization/transesterification exchange process when carried out with a large excess of diol. The dispersity of the TPC samples monotonically increases within each series with increasing FADD content. During transesterification and subsequent redistribution of the segments, a broadening of molar mass distributions occurs. Statistically, the extent of redistribution required to reach high molar mass increases with increasing FADD in the feed, and this may coincide with the small increase in $Đ$.

There are differences in the M_w between the samples, pointing toward a corresponding composition dependent viscosity−molar mass relationship (Table 1). Both series exhibit an incremental increase in M_w with increasing soft block content, ranging from 60−100 kg/mol. This trend is also suggestive of a stronger contribution to viscosity from the PET

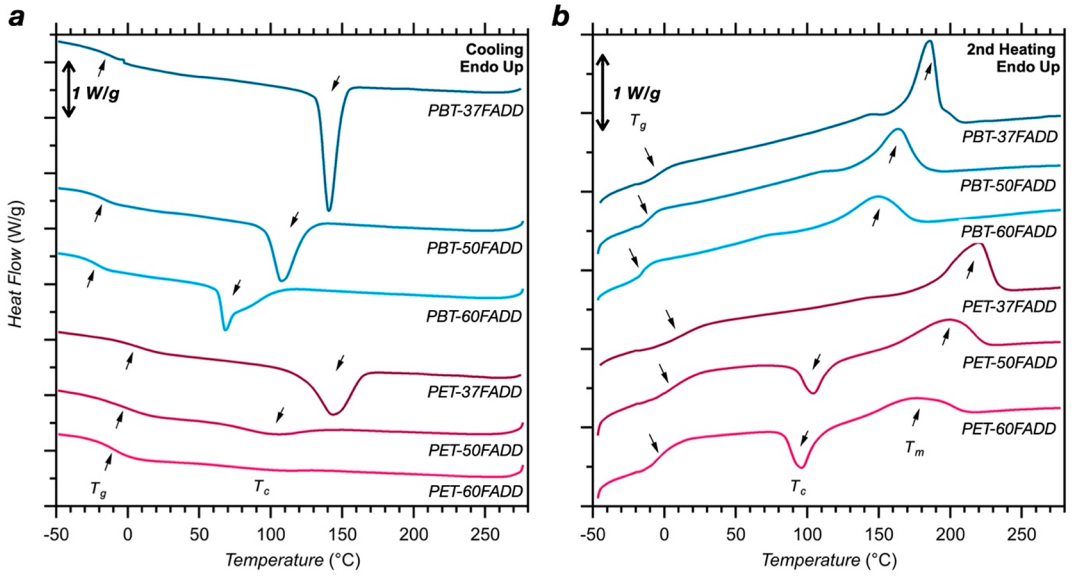

Figure 3. Thermograms for copolymer entries for (a) the cooling cycle (10 °C/min) and (b) the second heating cycle (10 °C/min). Thermograms have been shifted vertically for clarity, and approximate positions of thermal transitions have been indicated with arrows. Thermogram orientation is endo up.

https://doi.org/10.1021/acspolymersau.2c00019
ACS Polym. Au 2022, 2, 351−360

or PBT component.[39] Structurally, this makes sense considering the branched nature of the FADD blocks, with several short-chain hydrocarbon side groups on each repeating unit. This branched architecture is expected to lower the viscosity in the melt.[47,48] Therefore, samples enriched in FADD are anticipated to have a lower melt-viscosity at a given molar mass. In other words, a range of samples having approximately equal melt viscosity (i.e., torque−shear rate) would require higher molar mass from the samples with higher FADD content.

Thermal Properties

Samples were subjected to differential scanning calorimetry (DSC) to reveal the various thermally induced phase transitions (Figure 3). The thermal history was initially erased by heating the samples to 280 °C and annealing for 5 min, well above the nominal melting points and subsequently cooling and reheating at 10 °C/min, monitoring the heat flow. Notably, the rPET starting material is a homopolymer with a melting temperature of approximately 250 °C and crystallization temperature of approximately 195 °C as measured as the maxima in the thermograms from DSC (Figure S6). It has a crystallinity of ca. 30%, taking the melting enthalpy compared with a perfectly crystalline sample. Upon cooling, only one of the PET-based copolymers exhibits a pronounced crystallization event, with crystallization temperature (T_c) centered at 143 °C for PET-37FADD (see summary in Table 2). PET-37FADD is the richest in hard block, and the extensive crystallinity is consistent with the composition. This contrasts sharply with PET-based samples having larger amounts of soft block, in which very little crystallization takes place during cooling. Cooling of the PBT-based samples reveals starkly different crystallization behavior, during which all three samples exhibit pronounced crystallite development. The absolute enthalpy and T_c both decrease monotonically with decreasing hard block content, consistent with shorter segments and thus smaller crystallites. In any case, these thermograms indicate an unambiguous difference in molecular makeup, and are consistent with the chemical transformation according to ^{1}H NMR spectra. Further cooling to −50 °C followed by heating again to 280 °C reveals correspondingly marked differences in melting behavior. The PET-based copolymers each have a glass transition temperature (T_g) ranging from +4 °C for PET-60FADD to +13 °C for PET-37FADD. Further heating shows a melting transition (T_m) at 220 °C for PET-37FADD. However, the PET samples with increasing FADD content first undergo crystallization during heating, with T_c around 100 °C. This is consistent with our earlier work on PET-based copolyesters and suggests prohibitively slow crystallization kinetics that hinders crystallization during cooling before all molecular motion is frozen in place below the T_g.[25] Only after sufficient molecular mobility is regained at relatively high temperatures (i.e., above the T_g; > 70 °C) can the short PET segments arrange onto a lattice, which is accompanied by an exotherm. Further heating subsequently results in melting of the cold−crystallized spherulites, with broad endotherms and T_m falling between 170 and 200 °C for the two softer PET-FADD copolymers. The amount of crystallinity, reported in terms of percent crystallinity (X_c), has been assessed by normalizing relative to the PET-block content, compared with the extrapolated enthalpy for a perfectly crystalline PET homopolymer (ΔH_m° = 140 J g^{-1}).[49] The relative crystalline content ranges narrowly from 27−31%. The PBT-based samples do not crystallize upon heating, suggesting that the full extent of crystallinity was developed in the cooling cycle. The melting temperatures for PBT-copolymers with corresponding FADD-content are consistently lower than the PET-based counterparts, ranging from 148 to 184 °C. This is consistent with nearly complete chemical transformation of the hard block. Comparing the calculated X_c values for PBT-copolymers based on the enthalpy of perfectly crystalline PBT (ΔH_m° = 145 J g^{-1}) shows a range between 32−34%.[50] While the total amount of crystallinity is similar in the two different series, the kinetics of crystallization is unambiguously different. Furthermore, the T_g exhibited by the PBT-based copolyesters is consistently lower than the PET-based counterparts, occurring between −16 and −4 °C, again in line with the transformation in molecular makeup implied by molecular analysis. The occurrence of a single T_g in the segmented copolymers is not surprising considering the relative block lengths. Even highly incompatible segments would not be expected to extensively microphase separate with very low block molar mass (i.e., low segregation strength). Thus, a single T_g is in line with a single-phase system and the relative positions of the glass transitions are proportional to the relative T_g of the homopolymers of PET (+80 °C; Figure S6) and PBT (+60 °C).[51] Increasing FADD content, being relatively flexible, leads to decreasing glass transition temperatures in both series of TPCs. The contrasting thermal properties between the two series of copolyesters reveal important implications about the suitability for different applications. This suggests that the ability to transform PET to PBT using waste resources has major implications in terms of the utility of the resulting materials, which can be further validated by interrogating the mechanical performance.

Table 2. Thermal Characteristics Obtained from DSC Measurements[a]

entry	T_g (°C)	T_c (°C)	T_m (°C)	ΔH_m (J/g)	X_c (%)
PET-37DFA	13	143	220	27	31
PET-50DFA	5	102 (104)	198	22	31
PET-60DFA	4.2	101 (96)	173	15	27
PBT-37DFA	−4.4	141	184	31	34
PBT-50DFA	−9	107	163	23	32
PBT-60DFA	−16	68	148	19	33

[a]Thermal transitions and enthalpy values obtained from DSC thermograms. Composition determined from integration of signals from 1H NMR spectra. Crystallinity calculated from the composition and melting enthalpy values in reference to melting enthalpy of fully crystalline PET (ΔH_m° = 140 J g^{-1})[49] or fully crystalline PBT (ΔH_m° = 145 J g^{-1})[50] by $\alpha_c = \Delta H_m/(x\Delta H_m^\circ)$, where x is the weight fraction of PET.

Tensile Testing

Samples subjected to uniaxial tensile testing reveal marked differences between the PET and PBT-based copolymers, which can be connected to the contrasting crystalline content revealed by DSC measurements. Dumbbell samples were prepared by melt compression at 240 °C (see the Supporting Information for extensive sample preparation descriptions). A hydraulic melt press was used to create sheets (0.5 mm thickness), which were subsequently cooled quickly (≫10 °C/min). DSC thermograms captured from the pressed samples are consistent with amorphous PET-based copolymers and

https://doi.org/10.1021/acspolymersau.2c00019
ACS Polym. Au 2022, 2, 351−360

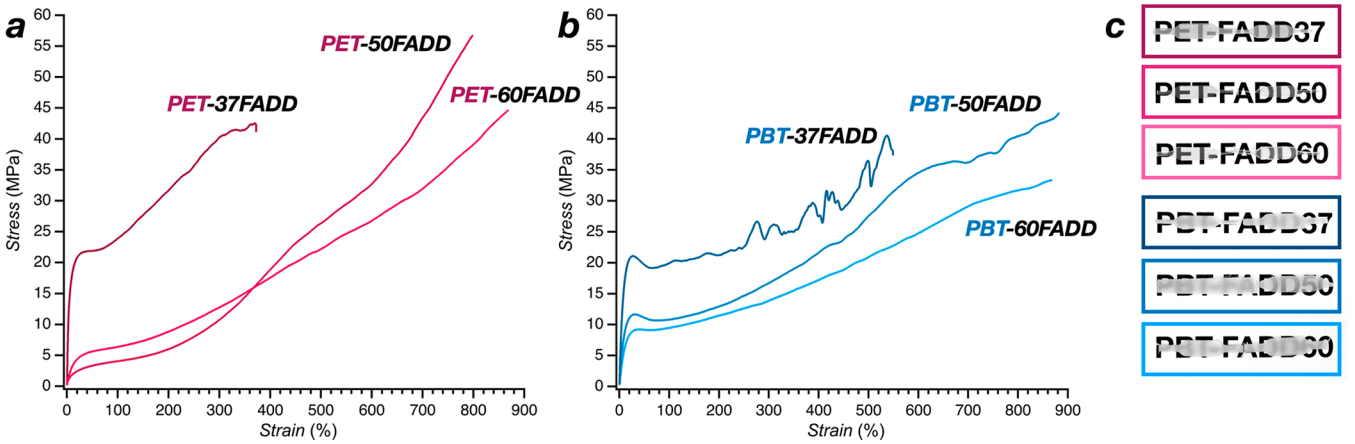

Figure 4. Summary of mechanical properties from tensile tests for (a) PET-based copolymers and (b) PBT-based copolymers. (c) Photographs of actual sample films (1 mm thick) placed over a paper with the sample name, highlighting the different opacity from crystallinity.

Table 3. Summary of Mechanical Properties Extracted from Tensile Testing and Dynamic Mechanical Analysis

entry	E (MPa)	stress at break (MPa)	strain at break (%)	G'@0 °C (MPa)	G'@20 °C (MPa)	G'@50 °C (MPa)
PET-37DFA	65.3 ± 4.4	35.5 ± 6.1	270 ± 90	1350	550	100
PET-50DFA	5.8 ± 0.7	52.4 ± 4.1	750 ± 35	1300	550	10
PET-60DFA	5.9 ± 0.5	39.2 ± 3.7	811 ± 43	260	60	30
PBT-37DFA	33.5 ± 1.4	38.1 ± 2.2	542 ± 6	1400	350	160
PBT-50DFA	15.1 ± 1.1	40.3 ± 3.1	852 ± 68	440	130	60
PBT-60DFA	8.1 ± 0.6	30.3 ± 3.6	831 ± 28	200	80	40

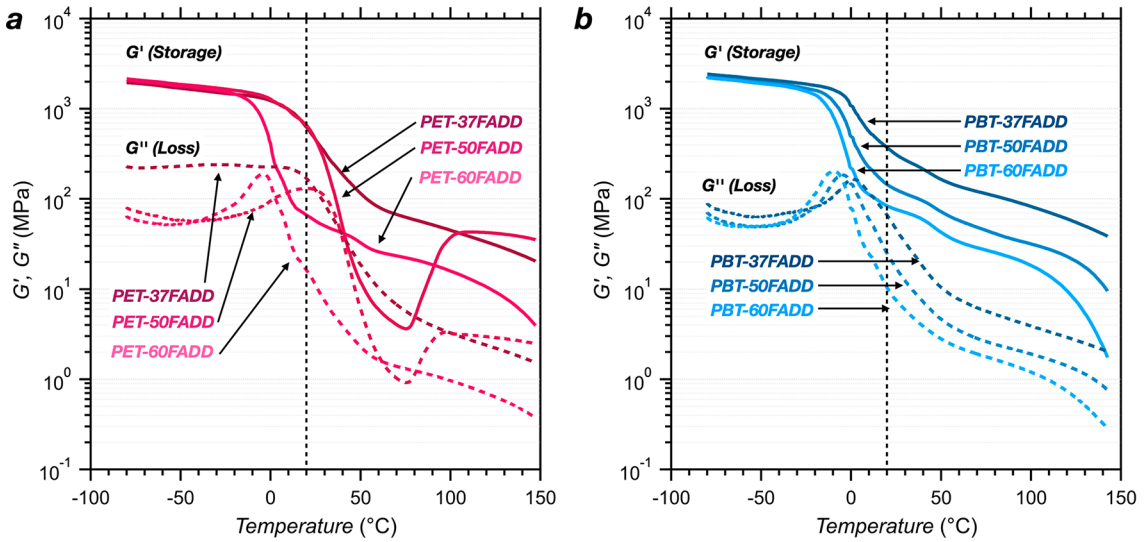

Figure 5. DMTA analysis from a temperature sweep (−80 to +150 °C) at 0.1% strain and 1 Hz frequency for (a) PET-based copolymers and (b) PBT-based copolymers, showing both the storage (G') and loss (G'') modulus. Vertical dashed line shows ambient temperature (20 °C) to aid with visual comparison.

semicrystalline PBT-based samples. Visually, the PBT-FADD samples were all opaque, while the PET-FADD samples were relatively transparent (Figure 4).

PET-37FADD has a relatively high modulus, which gives way to yielding and subsequent strain hardening, reaching an ultimate tensile stress of 35.5 ± 6.1 MPa (see Table 3). The average strain at break was 270 ± 90%. The two softer PET-FADD copolymers both exhibited significantly lower modulus and extensibility consistent with completely amorphous makeup. The Young's modulus for both PET-50FADD and PET-60FADD was approximately 6 MPa, while they both extended much further than the harder counterpart (elongation at break >750%). In contrast, the PBT samples all exhibited relatively high moduli and yielding, consistent with semicrystalline morphologies. The yield points monotonically decrease with decreasing PBT content. All samples exhibit significant ductility, extending >500% for PBT-37FADD and >800% for both PBT-50FADD and PBT-60FADD. Notably, PBT-37FADD shows multiple yielding during extension, which is likely an artifact of macroscopic crystalline alignment upon deformation. This unusual characteristic is nevertheless consistent with a significant amount of crystallinity and is thus consistent with the thermal attributes.

https://doi.org/10.1021/acspolymersau.2c00019
ACS Polym. Au 2022, 2, 351−360

Dynamic mechanical thermal analysis (DMTA) was used to probe more deeply into the mechanical features that distinguish the two chemically distinct hard blocks, elucidating the performance across a broad temperature window (Figure 5). The PET-based samples have distinct features that coincide with the thermal transitions observed in DSC thermograms. The peak in tan δ vs temperature plots points toward T_g values essentially in agreement with those measured by DSC (Figure S7). One exception is the PET-50FADD sample, which is convoluted by the cold crystallization behavior exhibited upon heating (vide infra). All PET-based samples exhibit a high stiffness ($G' \sim 2000$ MPa) between −80 and −10 °C, consistent with the material being completely glassy/crystalline. Each sample subsequently transitions to a rubbery material, with a transition temperature that increases with increasing FADD content. This transition occurs between −10 and +10 °C for PET-60FADD and slightly higher for PET-50FADD and PET-37FADD. The modulus of the rubbery plateau is lowest for the PET-60FADD, averaged over the full temperature scan. However, PET-50FADD notably undergoes a precipitous drop in storage modulus around +20 °C, ultimately showing a profile consistent with viscous relaxation and suggesting the absence of any physical cross-linking. In other words, it behaves as a viscous liquid without any crystallinity. Further heating results in an abrupt increase in G' starting at +75 °C, during which we posit that cold-crystallization occurs, brought on by the chain mobility afforded by elevated temperatures. Formation of the crystalline regions causes extensive physical cross-linking and a corresponding rubbery plateau around 40 MPa. Remarkably, PET-60FADD does not undergo a similar transition despite being more highly enriched in FADD soft-block. This may be attributed to a slightly different thermal history brought on by the sample preparation (hydraulic melt-press; see the Supporting Information).

PBT-based samples behave more predictably, without artifacts attributed to sample preparation and corresponding disparities in cooling rates that are linked to the (semicrystalline) morphologies. The stiffness at low temperature is essentially identical among all three samples, and comparable to PET-based copolymers. Between −80 and −25 °C, G' is approximately 2000 MPa. The subsequent transition temperatures going to the rubbery plateau gradually increase with increasing hard block (PBT) content. Likewise, G' in the rubbery plateau also increases with increasing PBT content, consistent with more rigidity owing to the larger crystalline content. Nevertheless, G' falls within a range of 20 to 200 MPa across the full temperature window (20−120 °C), exhibiting a remarkably wide useful temperature range with relatively high-performance characteristics. The exact stiffness and temperature profile are readily tuned by simple adjustments in the recipe.

CONCLUSION

We have shown a straightforward approach to expanding the utility of postconsumer waste rPET resources by chemical transformation via transesterification. In a single-pot synthetic setup performed fully in the melt, polycondensation/transesterification was conducted between a biobased fatty acid dimer diol and high molar mass rPET. The subsequent redistribution of these building blocks was aided by the addition of a small molecule diol, which promotes miscibility and enhances molecular mobility. Furthermore, the chemical structure of the small molecule additive was critically shown to determine the final polymer makeup. In this manner, analogous series of multiblock copolyesters were prepared with either rigid PET or PBT segments, arising from the addition of either EG or BDO, respectively. The polymer makeup was shown to have astounding implications on the thermal properties and the mechanical performance. Importantly, it has been shown that PET-based copolymers have significantly slower crystallization rates than the PBT-based counterparts. This has profound implications on the potential utility of these high-performance copolymers in applications that require injection molding, for example, where extremely fast cooling profiles are encountered during production cycles. This work uncovers a direct route to fast-crystallizing, mechanically robust segmented block polymers constructed nearly exclusively from sustainably sourced feedstocks (i.e., recyclate and renewables). We are keen to extend this principle to additional waste streams and targeting diverse architectural varieties.

ASSOCIATED CONTENT

Supporting Information

The Supporting Information is available free of charge at https://pubs.acs.org/doi/10.1021/acspolymersau.2c00019.

Materials, methods and synthetic procedures, additional SEC chromatograms from RI detector, ^{13}C NMR spectra for all copolymers, additional DMTA data, DSC thermograms (PDF)

AUTHOR INFORMATION

Corresponding Author

Louis M. Pitet − *Advanced Functional Polymers (AFP) Laboratory, Institute for Materials Research (IMO), Hasselt University, 3500 Hasselt, Belgium;* orcid.org/0000-0002-4733-0707; Phone: +32 11 26 83 20; Email: louis.pitet@uhasselt.be

Authors

Apostolos A. Karanastasis − *Advanced Functional Polymers (AFP) Laboratory, Institute for Materials Research (IMO), Hasselt University, 3500 Hasselt, Belgium;* orcid.org/0000-0001-9966-7873

Victoria Safin − *Advanced Functional Polymers (AFP) Laboratory, Institute for Materials Research (IMO), Hasselt University, 3500 Hasselt, Belgium*

Subin Damodaran − *Tosoh Bioscience, GmbH, 64347 Griesheim, Germany*

Complete contact information is available at: https://pubs.acs.org/10.1021/acspolymersau.2c00019

Notes

One of the authors is an employee of the company Tosoh, where the SEC analysis was performed.
The authors declare no competing financial interest.

ACKNOWLEDGMENTS

We greatly appreciate Greg Quintens (UHasselt) for assisting with SEC measurements and Guy Reggers for assisting with DMTA measurements. We gratefully acknowledge financial support from the Flemish Government and Flanders Innovation & Entrepreneurship (VLAIO) through the Moon-

shot project CoRe^2 (HBC2019.0116). Partial support is also appreciated from Hasselt University and the Research Foundation Flanders (FWO Vlaanderen) via the Hercules project AUHL/15/2-GOH3816N.

REFERENCES

(1) Geyer, R.; Jambeck, J. R.; Law, K. L. Production, use, and fate of all plastics ever made. *Sci. Adv.* **2017**, *3*, No. e1700782.
(2) Borrelle, S. B.; Ringma, J.; Law, K. L.; Monnahan, C. C.; Lebreton, L.; McGivern, A.; Murphy, E.; Jambeck, J.; Leonard, G. H.; Hilleary, M. A.; Eriksen, M.; Possingham, H. P.; De Frond, H.; Gerber, L. R.; Polidoro, B.; Tahir, A.; Bernard, M.; Mallos, N.; Barnes, M.; Rochman, C. M. Predicted growth in plastic waste exceeds efforts to mitigate plastic pollution. *Science* **2020**, *369*, 1515.
(3) Zheng, J.; Suh, S. Strategies to reduce the global carbon footprint of plastics. *Nat. Clim. Chang.* **2019**, *9*, 374.
(4) Lebreton, L.; Andrady, A. Future scenarios of global plastic waste generation and disposal. *Palgrave Commun.* **2019**, *5*, 6.
(5) Paszun, D.; Spychaj, T. Chemical Recycling of Poly(ethylene terephthalate). *Ind. Eng. Chem. Res.* **1997**, *36*, 1373−1383.
(6) Sinha, V.; Patel, M. R.; Patel, J. V. Pet Waste Management by Chemical Recycling: A Review. *J. Polym. Environ.* **2010**, *18*, 8−25.
(7) Ragaert, K.; Delva, L.; Van Geem, K. Mechanical and chemical recycling of solid plastic waste. *Waste Management* **2017**, *69*, 24−58.
(8) Tullo, A. PET recycling consortium grows. *Chem. Eng. News* **2019**, *97*, 12.
(9) Shojaei, B.; Abtahi, M.; Najafi, M. Chemical recycling of PET: A stepping-stone toward sustainability. *Polym. Adv. Technol.* **2020**, *31*, 2912−2938.
(10) Celik, G.; Kennedy, R. M.; Hackler, R. A.; Ferrandon, M.; Tennakoon, A.; Patnaik, S.; LaPointe, A. M.; Ammal, S. C.; Heyden, A.; Perras, F. A.; Pruski, M.; Scott, S. L.; Poeppelmeier, K. R.; Sadow, A. D.; Delferro, M. Upcycling single-use polyethylene into high-quality liquid products. *ACS Cent. Sci.* **2019**, *5*, 1795.
(11) Lewis, S. E.; Wilhelmy, B. E.; Leibfarth, F. A. Upcycling aromatic polymers through C-H fluoroalkylation. *Chem. Sci.* **2019**, *10*, 6270−6277.
(12) Tan, J. P. K.; Tan, J.; Park, N.; Xu, K. J.; Chan, E. D.; Yang, C.; Piunova, V. A.; Ji, Z. K.; Lim, A.; Shao, J. D.; Bai, A.; Bai, X. Y.; Mantione, D.; Sardon, H.; Yang, Y. Y.; Hedrick, J. L. Upcycling Poly(ethylene terephthalate) Refuse to Advanced Therapeutics for the Treatment of Nosocomial and Mycobacterial Infections. *Macromolecules* **2019**, *52*, 7878−7885.
(13) Jehanno, C.; Demarteau, J.; Mantione, D.; Arno, M. C.; Ruiperez, F.; Hedrick, J. L.; Dove, A. P.; Sardon, H. Selective Chemical Upcycling of Mixed Plastics Guided by a Thermally Stable Organocatalyst. *Angew. Chem., Int. Ed.* **2021**, *60*, 6710−6717.
(14) Guironnet, D.; Peters, B. Tandem Catalysts for Polyethylene Upcycling: A Simple Kinetic Model. *J. Phys. Chem. A* **2020**, *124*, 3935−3942.
(15) Vollmer, I.; Jenks, M. J. F.; Roelands, M. C. P.; White, R. J.; van Harmelen, T.; de Wild, P.; van der Laan, G. P.; Meirer, F.; Keurentjes, J. T. F.; Weckhuysen, B. M. Beyond Mechanical Recycling: Giving New Life to Plastic Waste. *Angew. Chem., Int. Ed.* **2020**, *59*, 15402−15423.
(16) Coates, G. W.; Getzler, Y. Chemical recycling to monomer for an ideal, circular polymer economy. *Nat. Rev. Mater.* **2020**, *5*, 501−516.
(17) Saint-Loup, R.; Robin, J. J.; Boutevin, B. Synthesis of poly(ethylene terephthalate)-block-poly (tetramethylene oxide) copolymer by direct polyesterification of reactive oligomers. *Macromol. Chem. Phys.* **2003**, *204*, 970−982.
(18) Ghassemi, H.; Schiraldi, D. A. Thermoplastic Elastomers Derived from Bio-Based Monomers. *J. Appl. Polym. Sci.* **2014**, *131*, 39815.
(19) Rorrer, N. A.; Nicholson, S.; Carpenter, A.; Biddy, M. J.; Grundl, N. J.; Beckham, G. T. Combining Reclaimed PET with Bio-based Monomers Enables Plastics Upcycling. *Joule* **2019**, *3*, 1006−1027.
(20) Akato, K. M.; Nguyen, N. A.; Bonnesen, P. V.; Harper, D. P.; Naskar, A. K. Recycling Waste Polyester via Modification with a Renewable Fatty Acid for Enhanced Processability. *ACS Omega* **2018**, *3*, 10709−10715.
(21) Gioia, C.; Vannini, M.; Marchese, P.; Minesso, A.; Cavalieri, R.; Colonna, M.; Celli, A. Sustainable polyesters for powder coating applications from recycled PET, isosorbide and succinic acid. *Green Chem.* **2014**, *16*, 1807−1815.
(22) Gioia, C.; Minesso, A.; Cavalieri, R.; Marchese, P.; Celli, A.; Colonna, M. Powder coatings for indoor applications from renewable resources and recycled polymers. *J. Coat. Technol. Res.* **2015**, *12*, 555−562.
(23) Waskiewicz, S.; Langer, E. Synthesis of new oligoesterdiols based on waste poly(ethylene terephthalate) and dimerized fatty acid. *Polymer* **2021**, *227*, 123832.
(24) Langer, E.; Waskiewicz, S.; Lenartowicz-Klik, M.; Bortel, K. Application of waste poly(ethylene terephthalate) in the synthesis of new oligomeric plasticizers. *Polym. Degrad. Stab.* **2015**, *119*, 105−112.
(25) Karanastasis, A. A.; Safin, V.; Pitet, L. M. Bio-Based Upcycling of Poly(ethylene terephthalate) Waste for the Preparation of High-Performance Thermoplastic Copolyesters. *Macromolecules* **2022**, *55*, 1042−1049.
(26) Fakirov, S. Condensation Polymers: Their Chemical Peculiarities Offer Great Opportunities. *Prog. Polym. Sci.* **2019**, *89*, 1−18.
(27) Walkowiak, K.; Irska, I.; Zubkiewicz, A.; Rozwadowski, Z.; Paszkiewicz, S. Influence of Rigid Segment Type on Copoly(ether-ester) Properties. *Materials* **2021**, *14*, 4614.
(28) Baeza, G. P. Recent advances on the structure-properties relationship of multiblock copolymers. *J. Polym. Sci.* **2021**, *59*, 2405−2433.
(29) Hao, T. H.; Zhang, C.; Hu, G. H.; Jiang, T.; Zhang, Q. C. Effects of co-hard segments on the microstructure and properties thermoplastic poly(ether ester) elastomers. *J. Appl. Polym. Sci.* **2016**, *133*, 43337.
(30) Fakirov, S.; Gogeva, T. Poly(Ether Ester)S Based on Poly(Butylene Terephthalate) and Poly(Ethylene Glycol).1. Poly(Ether Ester)S with Various Polyether - Polyester Ratios. *Makromol. Chem., Macromol. Chem. Phys.* **1990**, *191*, 603−614.
(31) Fakirov, S.; Gogeva, T. Poly(Ether Ester)S Based on Poly(Butylene Terephthalate) and Poly(Ethylene Glycol),.2. Effect of Polyether Segment Length. *Makromol. Chem., Macromol. Chem. Phys.* **1990**, *191*, 615−624.
(32) Chi, D. Q.; Liu, F.; Na, H. N.; Chen, J.; Hao, C. C.; Zhu, J. Poly(neopentyl glycol 2,5-furandicarboxylate): A Promising Hard Segment for the Development of Bio-based Thermoplastic Poly(ether-ester) Elastomer with High Performance. *ACS Sustainable Chem. Eng.* **2018**, *6*, 9893−9902.
(33) Vendamme, R.; Olaerts, K.; Gomes, M.; Degens, M.; Shigematsu, T.; Eevers, W. Interplay Between Viscoelastic and Chemical Tunings in Fatty-Acid-Based Polyester Adhesives: Engineering Biomass toward Functionalized Step-Growth Polymers and Soft Networks. *Biomacromolecules* **2012**, *13*, 1933−1944.
(34) Nurhamiyah, Y.; Amir, A.; Finnegan, M.; Themistou, E.; Edirisinghe, M.; Chen, B. Q. Wholly Biobased, Highly Stretchable, Hydrophobic, and Self-healing Thermoplastic Elastomer. *ACS Appl. Mater. Interfaces* **2021**, *13*, 6720−6730.
(35) Maisonneuve, L.; Lebarbé, T.; Grau, E.; Cramail, H. Structure-properties relationship of fatty acid-based thermoplastics as synthetic polymer mimics. *Polym. Chem.* **2013**, *4*, 5472−5517.
(36) Kwiatkowska, M.; Kowalczyk, I.; Kwiatkowski, K.; Szymczyk, A.; Roslaniec, Z. Fully biobased multiblock copolymers of furan-aromatic polyester and dimerized fatty acid: Synthesis and characterization. *Polymer* **2016**, *99*, 503−512.
(37) Kwiatkowska, M.; Kowalczyk, I.; Szymczyk, A. Poly(ethylene furanoate) modified with dimerized fatty acid diol towards multiblock copolymers: Microstructure - Property relationship. *Mater. Today Commun.* **2019**, *20*, 100577.

https://doi.org/10.1021/acspolymersau.2c00019
ACS Polym. Au 2022, 2, 351−360

(38) Kwiatkowska, M.; Kowalczyk, I.; Kwiatkowski, K.; Szymczyk, A.; Jedrzejewski, R. Synthesis and structure - property relationship of biobased poly(butylene 2,5-furanoate) - block - (dimerized fatty acid) copolymers. *Polymer* **2017**, *130*, 26−38.
(39) Lim, H. C. A. Thermoplastic Polyesters. In *Brydson's Plastics Materials*, Eighth ed.; Gilbert, M., Ed.; Butterworth-Heinemann: 2017; Chapter 20, pp 527−543.
(40) Gilbert, M.; Hybart, F. J. Effect of chemical structure on crystallization rates and melting of polymers: Part 1. Aromatic polyesters. *Polymer* **1972**, *13*, 327−332.
(41) El Fray, M.; Slonecki, J. Dimer fatty acid-modified poly[ester-b-ether]s: Synthesis and properties. *Polym.-Plast. Technol. Eng.* **1999**, *38*, 51−69.
(42) El Fray, M.; Skrobot, J.; Bolikal, D.; Kohn, J. Synthesis and characterization of telechelic macromers containing fatty acid derivatives. *React. Funct. Polym.* **2012**, *72*, 781−790.
(43) Gubbels, E.; Jasinska-Walc, L.; Merino, D. H.; Goossens, H.; Koning, C. Solid-State Modification of Poly(butylene terephthalate) with a Bio-Based Fatty Acid Dimer Diol Furnishing Copolyesters with Unique Morphologies. *Macromolecules* **2013**, *46*, 3975−3984.
(44) Manuel, H. J.; Gaymans, R. J. Segmented block copolymers based on dimerized fatty acids and poly(butylene terephthalate). *Polymer* **1993**, *34*, 636−641.
(45) Agarwal, P.; Cohoon, K.; Dhawan, S.; Gallucci, R. R.; Kannan, G.; Miller, K. F.; Shah, D. Process for making polybutylene terephthalate (PBT) from polyethylene terephthalate (PET). US 2011/0124821 A1, May 26, 2011.
(46) Gupta, V. B.; Bashir, Z. PET Fibers, Films, and Bottles: Sections 1−4.13. *Handbook of Thermoplastic Polyesters* **2002**, 317−361.
(47) Munari, A.; Pilati, F.; Pezzin, G. A study on the melt viscosity of linear and branched poly(butyleneterephthalate). *Rheol. Acta* **1984**, *23*, 14−19.
(48) Moore Jr, L. D. Relations among melt viscosity, solution viscosity, molecular weight, and long-chain branching in polyethylene. *J. Polym. Sci.* **1959**, *36*, 155−172.
(49) Vilanova, P. C.; Ribas, S. M.; Guzman, G. M. Isothermal crystallization of poly(ethylene-terephthalate) of low molecular weight by differential scanning calorimetry: 1. Crystallization kinetics. *Polymer* **1985**, *26*, 423−428.
(50) Fakirov, S.; Apostolov, A. A.; Boeseke, P.; Zachmann, H. G. Structure of Segmented Poly (Ether Ester)s as Revealed by Synchrotron Radiation. *J. Macromol. Sci., Phys.* **1990**, *B29*, 379−395.
(51) Fakirov, S.; Gogeva, T. Poly(Ether Ester)s Based on Poly(Tetramethylene Terephthalate) and Poly(Ethylene Glycol).3. Effect of Thermal-Treatment and Drawing on the Structure of the Poly(Ether Ester)S. *Makromol. Chem., Macromol. Chem. Phys.* **1990**, *191*, 2341−2354.

https://doi.org/10.1021/acspolymersau.2c00019
ACS Polym. Au 2022, 2, 351−360